Plasma-activated catalytic formation of ammonia from N_2-H_2: Influence of temperature and noble gases addition

M. Ben Yaala[1,2], D-F. Scherrer[1], A. Saeedi[1], L. Moser[1], K. Soni[1], R. Steiner[1], G. De Temmerman[3], M. Oberkofler[4], L. Marot[1] and E. Meyer[1]

[1] Department of Physics, University of Basel, Klingelbergstrasse 82, CH-4056 Basel, Switzerland

[2] Department of Biomedical Engineering, University of Strathclyde, Glasgow G1 1QE, United Kingdom

[3] ITER Organization, Route de Vinon-sur-Verdon, CS 90 046, 13067 St Paul Lez Durance Cedex, France

[4] Max Planck Institute for Plasma Physics, Boltzmannstrasse 2, 85748 Garching, Germany

E-mail: marwa.benyaala@unibas.ch/marwa.ben-yaala@strath.ac.uk

Abstract. In the ITER tokamak, injection of nitrogen is foreseen to decrease the heat loads on the divertor surfaces. However, once dissociated, nitrogen atoms react with hydrogen isotopes to form ammonia isotopologues. The formation of tritiated ammonia may pose some issues with regards to tritium inventory and operation duty cycle. In this paper, we report a study of the effect of three parameters of relevance for the fusion environment on the ammonia production, including the presence of a catalytic surface, sample temperature and noble gas addition. Results of ammonia formation from N_2/H_2 RF plasma (both with and without tungsten or stainless steel surface) show the importance of the presence of a catalyst in the ammonia formation process. By increasing the temperature of the W samples up to 1270 K, ammonia formation demonstrated a continuous decrease due to two major factors. For high temperatures above 650 K and 830 K, for stainless steel and W, respectively, the reduction results from the thermal decomposition of ammonia. For the lower temperature range, the temperature rise leads to the formation of more stable nitrides that do not tend to react further with hydrogen to form NH_2 and NH_3. Interestingly, the addition of helium or argon to the N_2/H_2 plasma show opposite effects on the ammonia production. He effectively decreases the percentage of NH_3 by acting as a barrier for the surface processes. On the other hand, argon impacts more the plasma processes probably by increasing the active nitrogen species in the plasma and as a consequence the percentage of formed ammonia.

1. Introduction

In fusion devices, extrinsic impurities are typically injected in the edge region of the confined plasma to help dissipate the intense power exhausting the plasma before it reaches nearby surfaces. In particular, for burning plasma conditions in ITER, a high divertor radiation level will be mandatory to avoid thermal overload of divertor components. Seeding gases that are currently under investigation for different Tokamaks are nitrogen (N_2), neon (Ne) and argon (Ar). N_2 is the preferred species for existing devices because of its favorable radiative properties as well as its beneficial effect on the plasma performances [1, 2]. However, once dissociated, N atoms chemically react with H and its isotopes (D/T) to form ammonia (NH_3) isotopologues. The assessment of ammonia formation in tokamaks is still very difficult and subjected to an internal debate. In ASDEX-Upgrade(Axially Symmetric Divertor Experiment), the formation of ammonia during nitrogen-seeded discharges has been investigated by analyzing the exhaust gases using mass spectrometers [1, 3–7]. It was found that up to 8 % of the injected N_2 was converted into NH_3. The interpretation of this results was challenging due to the additional presence of water and methane and due to isotope exchange reactions of deuterated ammonia with H in the pump ducts that lead to the spectrometers. Indeed, the data were obtained following other experiments where the wall loading was not controlled and identified at the start of the series and the spectrometer did not reach its optimal performance [3]. In JET (Joint European Torus), 15 % of the injected N_2 was transformed into NH_3 [8] and this value is also uncertain due to the difficult calibration of the diagnostics used to detect ammonia. The formation of tritiated ammonia in future fusion devices such as ITER may pose some issues with regards to tritium inventory and duty cycle. In this context, ammonia formation has become an increasingly important subject of research for the nuclear fusion community in the past few years [1, 2, 4, 6]. In particular, the fundamental understanding of the impact of specific parameters from the fusion reactor environment on the ammonia formation process would be the key to both predict the quantity of ammonia that might be formed in ITER and to find possible ways to decrease it [9–11].

In the present article, we demonstrate the effect of three parameters on the ammonia production from N_2/H_2 plasma including the presence of a catalytic surface, sample temperature and He or Ar addition. Two fusion relevant materials playing the role of catalysts for the ammonia production were investigated: tungsten (W) and stainless steel (SS). While the W constitutes the divertor surface material in ITER, the SS is used for the vacuum vessel, the divertor cassettes, the shield block and the Port Plug front surface. The study was initially performed at room temperature (RT) for both surfaces and then for increasing temperature up to 1270 K. This highest temperature value is relevant for the ITER divertor and in particular for the divertor active areas where the plasma impact occurs [12]. The effects of helium and argon on the ammonia formation are also investigated in this paper. He will, in fact, be present in ITER as the ash of the fusion reaction. Argon, on the other hand, was identified as the best

candidate for the simultaneous enhancement of core and divertor radiation [2] in the case where an elevated main chamber radiation is desired as well. Although this gas is not foreseen to be used in ITER to avoid high core level contamination, the use of argon will be required in the future DEMO prototype reactor to insure a high main plasma radiation level.

Our studies were performed in a newly built setup, with the specificity of being a quartz vacuum chamber (no metal) to avoid the retention of the formed ammonia on the reactor wall [13]. In another conventional stainless steel vacuum chamber, surface chemistry analysis were carried out in vacuo using X-ray photoelectron spectroscopy (XPS).

2. Experimental procedure

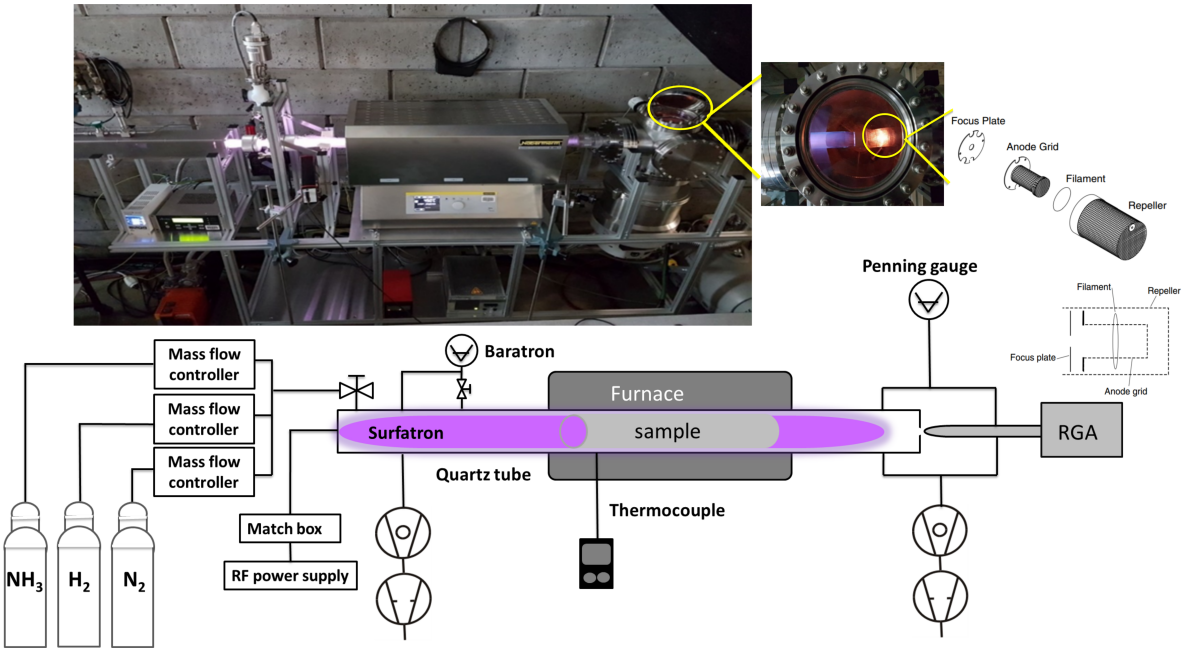

Figure 1: Schematic and real picture (on top) of the RF plasma reactor and surrounding equipment for gas inlet and outlet

The experiments were performed in an in-house built metal free reactor shown in Figure 1. A detailed description of the system, as well as the calibration procedure, can be found in [14]. Briefly, this setup consists of a cylindrical quartz tube connected to a waveguide surfatron plasma source. Processing gases are introduced to the reaction chamber using mass flow controllers and the plasma is created in the tube through a matching network by a 13.56 MHz radio frequency generator at a typical power of 120 W. Inside the tube a rolled catalyst foil is placed and can be heated with a furnace. The two catalysts used in this study are W (purity 99.97 %) and SS (mass percent composition shown in Table 1). The average roughness (Ra) of both catalysts was measured using

a Tencor Alpha Step 500 Surface Profilometer. The SS and W Ra values are 69 nm and 190 nm, respectively. On the other side of the quartz tube, a quadrupole mass spectrometer (SRS Residual Gas Analyser RG A200) is connected through a 2 mm diameter pinhole. The RGA is used for both qualitative and quantitative analyses of gas species resulting from the plasma. In order to get a good background pressure of around 8×10^{-9} mbar in the RGA chamber, the system is pumped from two sides through a turbo and a primary pump. However during the plasma process, gases are pumped only through the RGA chamber in order to detect all gas species. The resulting typical pressure value is around of 5×10^{-6} mbar which corresponds to 2×10^{-2} mbar in the quartz reactor.
A wall conditioning step using pure Ar plasma is carried out before each experiment to remove the contaminants adsorbed on the reactor wall. In particular, residual water can be efficiently removed and the measured water content was below 2 % of the total gas mixture during the full process. The calibration of the RGA is then performed by determining the cracking patterns (CP) and the calibration factors (CF) for species present in the plasma (N_2, H_2, NH_3, Ar, He and H_2O). CFs represent the proportionality factor of the measured detected current in the RGA and its known partial pressure. CPs, on the other hand, represent the ratio between the major peak intensity and the other fragments intensity created by electron impact ionization in the RGA.

Element	Fe	Cr	Ni	Mo	Mn	Si	N	P	C	S
%	69.52	16.9	10.1	2.08	1.74	0.46	0.048	0.032	0.019	0.001

Table 1: Chemical composition of the stainless steel foil

In this paper, three parameters influencing the ammonia production are studied including the catalyst material, the surface temperature and the presence of helium and argon. To investigate the catalytic surface effect, the experiment was conducted by introducing N_2 and H_2 at different ratios. The N_2 initial concentration (X_{N_2}) defined as the ratio between N_2 initial partial pressure (P_{N_2}) and the total pressure (P_{tot}) was varied from 1 to 80 % in the N_2/H_2 mixture and the total pressure was kept constant (P_{tot}=2×10^{-2} mbar). Prior to the plasma ignition, no ammonia was observed in the RGA for the different N_2/H_2 gas mixtures. The plasma was then ignited for 5 to 10 min when no catalyst was introduced in the tube and for 15 min in the presence of the sample which represents the time needed to reach the reaction equilibrium state [14]. When Ar or He were used, a constant ratio of 1/9 of N_2/H_2 (X_{N_2}/X_{H_2}=1/9) was fixed for a P_{tot}=2×10^{-2} mbar. All experiments were repeated at least twice (later on the error bars represent the standard deviation of the measurements) and a reference experiment for an X_{N_2} of 10 % is repeated after each experimental day to ensure that the status of the catalyst surfaces does not change over time. The decomposition procedure of the measured spectra was described in our previous paper [14].

Chemical analyses were performed in vacuo by XPS (procedure described in [14]

after plasma exposure in another conventional SS vacuum chamber to characterize the surface state. Prior to the XPS measurements, a 20-nm tungsten film was deposited by pulsed-DC magnetron sputtering [15] and then exposed to N_2/H_2 (1/9) plasma for 20 minutes at 1.2×10^{-2} mbar under the following conditions:
(i) plasma exposure on a non heated sample (RT) first and then on hot surfaces (406 K and 513 K).
(ii) Ar and He were mixed with N_2 and H_2 at two fractions (20 and 50 %) both at RT. For each of these XPS measurements, a new sample is loaded and a fresh W deposition is performed.

3. Results

3.1. Effect of the catalytic material (W, SS) on the ammonia formation

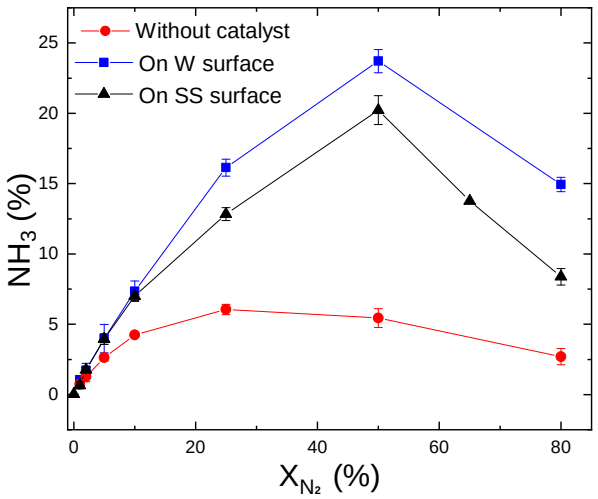

Figure 2: Ammonia production without catalyst (red curve), on W (black curve) and on SS (green) catalyst at RT for different X_{N_2}

Figure 2 shows the ammonia percentage (defined as the ratio between its partial pressure (P_{NH_3}) and P_{tot} during the plasma) against X_{N_2} without and with catalyst (W and SS). In the absence of catalyst, the ammonia production increases up to 6 % with increasing X_{N_2} up to 25 % that corresponds to the stoichiometric composition of nitrogen in ammonia. By introducing a catalytic surface, we noticed an increase of the NH_3 production up to 20 and 24 % for SS and W, respectively and a shift of these values to higher X_{N_2} (Figure 2).

3.2. Temperature effect

3.2.1. Ammonia formation at high temperature

The effect of surface temperature (T_{Surf}) on the ammonia formation rate was studied

in the range RT to 1273 K.

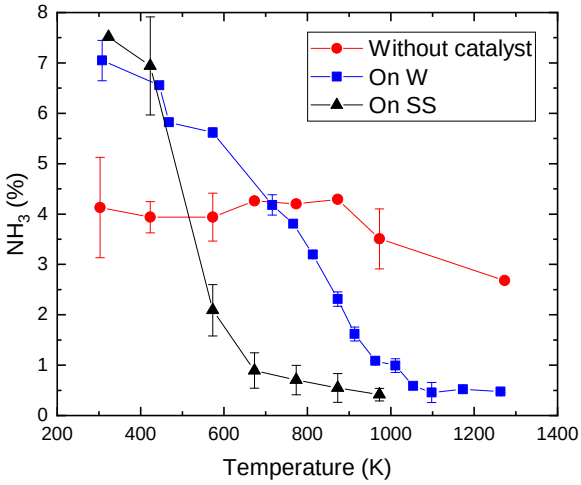

Figure 3: Effect of T_{Surf} on ammonia production from N_2/H_2 (1/9) plasma for different catalytic materials

In the absence of catalyst, the ammonia formation rate was almost constant up to 870K and then slightly decreased from 4.2 % to 2.7 % for higher temperatures. When a catalyst is used, a strong effect of T_{Surf} is observed. For both W and SS surfaces the NH_3 fraction decreases as soon as T_{Surf} is increased. Yet a clear difference can be observed between the two materials. On the SS surface, the NH_3 percentage drops drastically between 400 and 700 K and is very low for higher temperatures. For W, the effect of T_{Surf} is more gradual and the formation rate remains higher than for SS up to 1100 K, after which does not evolve anymore.

3.2.2. Thermal decomposition of the ammonia gas

The thermal decomposition of pure NH_3 gas without plasma was then studied as a function of temperature by flowing the ammonia gas at fixed pressure inside the quartz tube for different materials. The temperature was continuously increased up to 1273 K and the resulting peaks from the decomposition were recorded by the RGA on the other side of the tube.

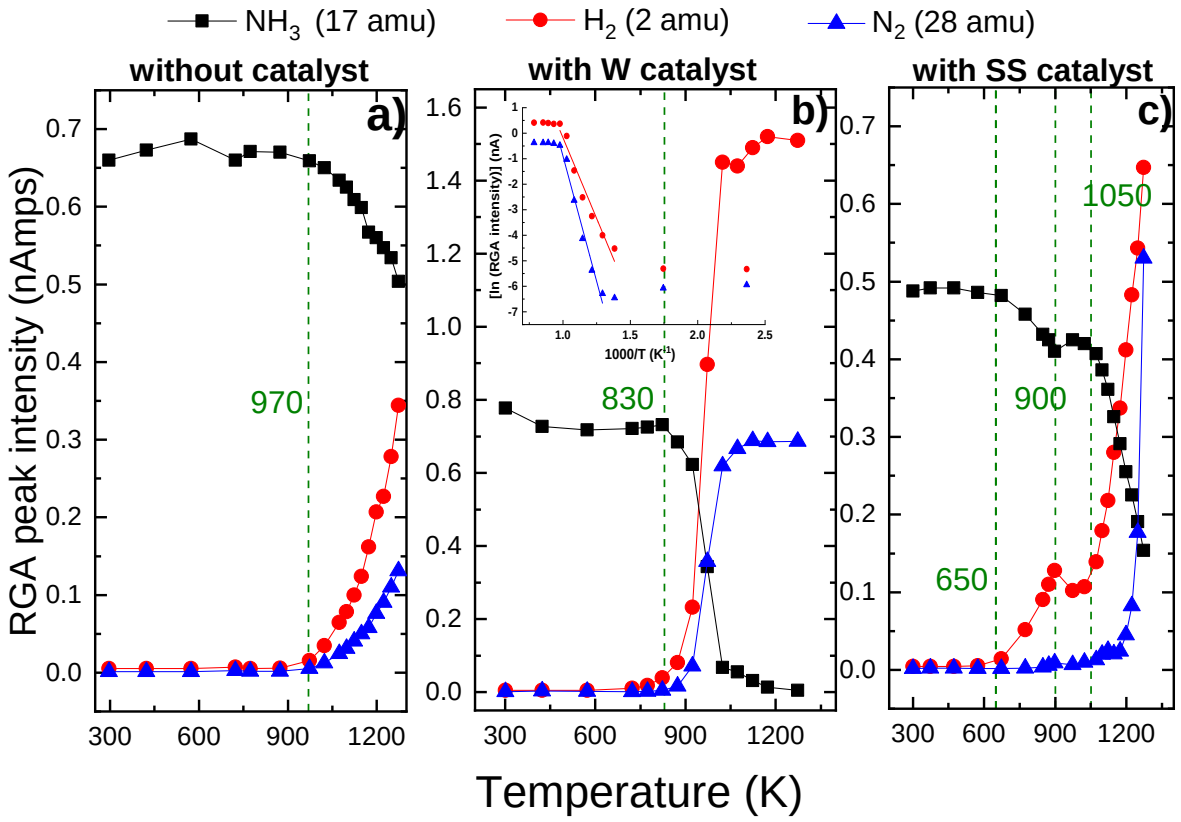

Figure 4: Variation of the RGA peak intensities of the H_2, NH_3 and N_2 at 2, 17 and 28 amu respectively due to the ammonia thermal decomposition a) without catalyst b) on W surface and c) on SS surface. The inset of b) represents the logarithm of H_2 and N_2 peak intensities plotted versus inverse temperature values.

Figure 4 shows the variation of the major RGA peaks of NH_3 (17 amu), H_2 (2 amu) and N_2 (28 amu) as a function of the temperature. Comparing the effect of the three materials, it is seen that the decomposition of ammonia into N_2 and H_2 starts at different temperatures. Without catalyst, ammonia starts to decompose into nitrogen and hydrogen at 970 K. The decomposition was partial under these conditions even for the highest measured temperature and only 23 % of the initial amount was decomposed. On the W surface, the decomposition initiates at around 830 K. For temperatures between 830 and 1023 K, the ammonia peak intensity drops drastically while simultaneously both nitrogen and hydrogen peaks rise to near their maximum values. The SS surface, on the other hand, seems to be more efficient towards the NH_3 decomposition which started at lower temperature than W (650 vs 830 K). As can be observed, ammonia thermal decomposition to nitrogen and hydrogen exhibit a particular trend on this surface. Remarkably, the 17 amu peak of NH_3 slightly decreases from 650 to 900 K followed by the release of only hydrogen (no nitrogen), increases back from 900 to 1050 K and decreases with a faster rate for higher temperature values. The N_2 release increase is shifted to higher temperature above 1050 K.

3.2.3. Chemical species formed on the surface after plasma exposure: XPS studies
Four elements were identified by XPS on the W plasma exposed samples: tungsten, nitrogen as well as oxygen and carbon contaminants. Despite the use of our cold liquid nitrogen (LN_2) trap, the presence of oxygen (3 to 9 atomic percent concentration (at.%)) and carbon (around 2 at.%) could not be avoided. These species are typically adsorbed during the time required for the transfer to the XPS chamber and/or during the cool down of the sample (maximum 30 min).

Figure 5 represents the N1s core level spectra measured after N_2/H_2 plasma exposures of the W surface at three different temperatures. The total nitrogen atomic concentration on the surface as well as its decomposition fraction into N/NH (at 397.6 eV), NH_2 (at 398.5 eV) and NH_3 (at 400.4 eV) are presented. The total relative error on each concentration value was assumed to be 15% according to previous literature report [16].

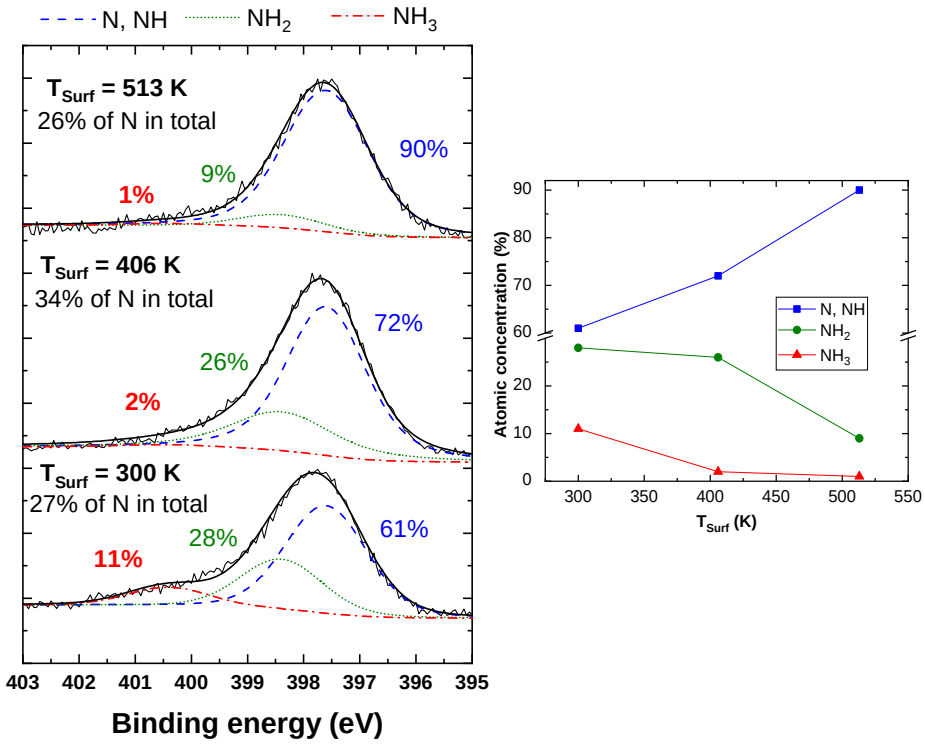

Figure 5: (Left) N1s core levels spectra recorded after N_2/H_2 plasma exposure of the W surface at 300, 406 and 513 K. The red (dashdotted), green (shortly dotted) and blue (dashed) curves are the individual chemical states. Solid black curves are the raw data and the sum curves. (Right) Relative N, NH, NH_2 and NH_3 atomic concentration as a function of T_{Surf}

Comparing the evolution of the three peaks for increasing T_{surf}, it can be observed that both NH_3 and NH_2 peaks drop drastically from 11 to 1 at.% and 28 to 9 at.%, respectively while the N/NH peak rises up to 90 at.% from the total nitrogen peak on the surface. W4f core level spectra of the exposed W sample to N_2/H_2 plasma show

also a nitride formation (WN and WN_2). The spectrum was presented in Figure 6 of our last paper [14].

3.3. Influence of Ar and He addition

3.3.1. Influence of Ar and He addition on ammonia formation

In order to investigate the effect of noble gases addition on the ammonia formation, He or Ar gas was mixed with N_2 and H_2 at a fixed P_{tot} (2×10^{-2} mbar) and fixed X_{N_2}/X_{H_2} (1/9). As P_{tot} of the three gases should be kept constant during the process, increasing the Ar or He content would imply to decrease the nitrogen and hydrogen concentrations and as a consequence the formed ammonia. One way to correct this effect can be achieved by normalizing the NH_3 formed amount to the initial N_2+H_2 content from P_{tot}. This normalization is valid if the ammonia formation would only depend on X_{N_2}/X_{H_2} and not on their pressure. To validate this assumption, an experiment devoted to study the influence of P_{tot} on ammonia formation was conducted by keeping the X_{N_2}/X_{H_2} constant and increasing their partial pressure. Figure 6a shows a nearly constant formation of ammonia for a P_{tot}= P_{N_2}+P_{H_2} varied between 1×10^{-2} and 5×10^{-2} mbar allowing therefore to study the Ar and He effects using the above-mentioned approach.

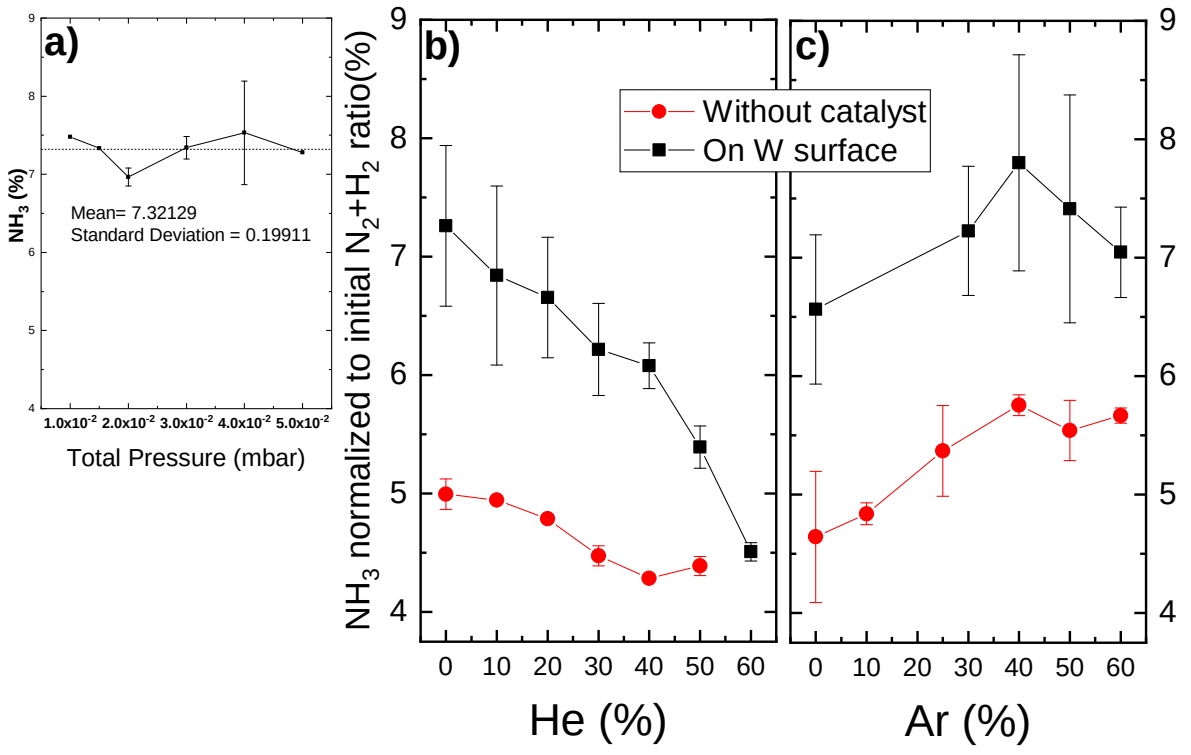

Figure 6: Impact of the a) gas total pressure b) helium admixture and c) argon admixture on the ammonia production

Ammonia production results without catalyst and on W surface are presented in Figure 6b and Figure 6c for several He and Ar percentages up to 60 %. For instance,

the highest introduced argon or helium percentage (60 %) corresponds to P_{Ar} or P_{He} = 1.2×10^{-2} mbar and P_{N_2}+P_{H_2} = 8×10^{-3} mbar while the lower noble gas inlet concentration (10 %) corresponds to P_{N_2}+P_{H_2} = 1.8×10^{-2} mbar.
Two opposite effects can be seen for the two noble gases. Up to 40 % of argon addition, the ammonia production slightly increases both without and with W catalyst. Meanwhile, it decreases by increasing the He percentage in the gas mixture and in particular on the tungsten where a significant drop can be seen.

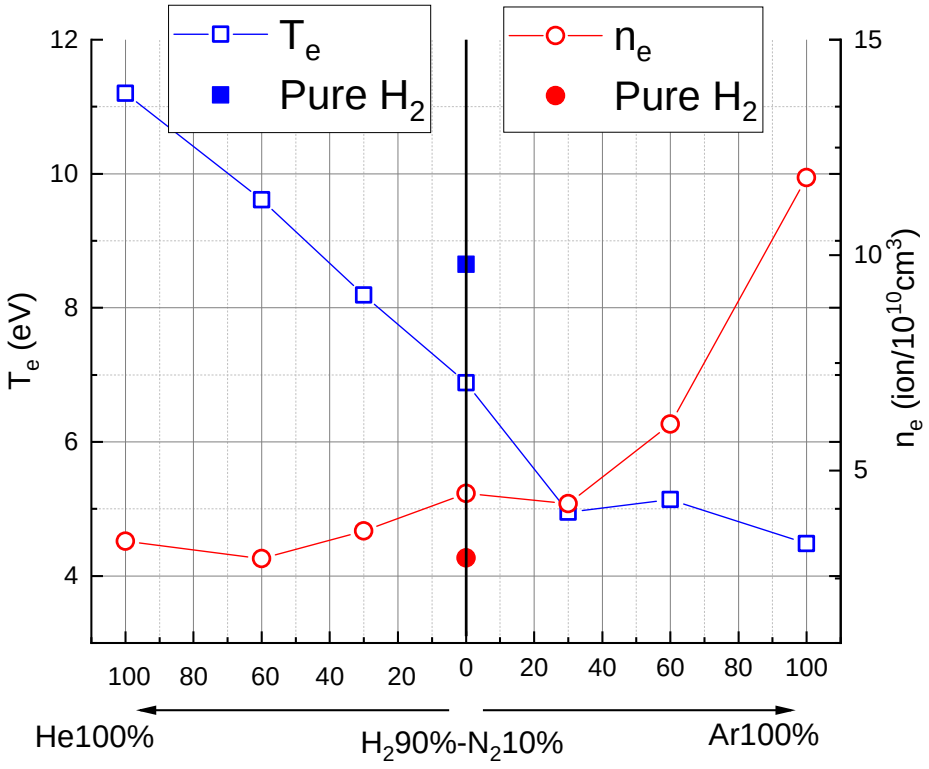

Figure 7: Electron temperature T_e (blue) and density n_e (red) variation with helium and Ar percentage in the N_2/H_2 mixture. Plasma parameters (T_e and n_e) are also represented for pure hydrogen plasma

.

The electron temperature (T_e) and electron density (n_e) are measured using a Langmuir probe for pure H_2, N_2/H_2 and several mixtures of He or $Ar/N_2/H_2$ plasmas. The results are represented in Figure 7. While the addition of He highly increases T_e and slightly n_e, the Ar increasing content impacts more the electron density than the electron temperature.

3.3.2. Influence of Ar and He addition on surface species

After the exposure at RT of several samples coated with W to N_2/H_2 + Ar or He plasma in the metallic chamber, the samples were analyzed by XPS. Measurements revealed the existence of three species on the samples: tungsten (63-69 % atomic concentration),

nitrogen (28-33 at.%) and oxygen contaminants (less than 5 at.%). Figure 8 represents the N1s core level spectra resulting from a pure N_2/H_2 as well as N_2/H_2/Ar or He plasma exposure of the surface. X_{N_2}/X_{H_2} was kept constant and 2 different fractions of the noble gases were added (20 and 50 %). In order the study the impact of lower fraction of He and Ar on the ammonia production, further experiments are required.

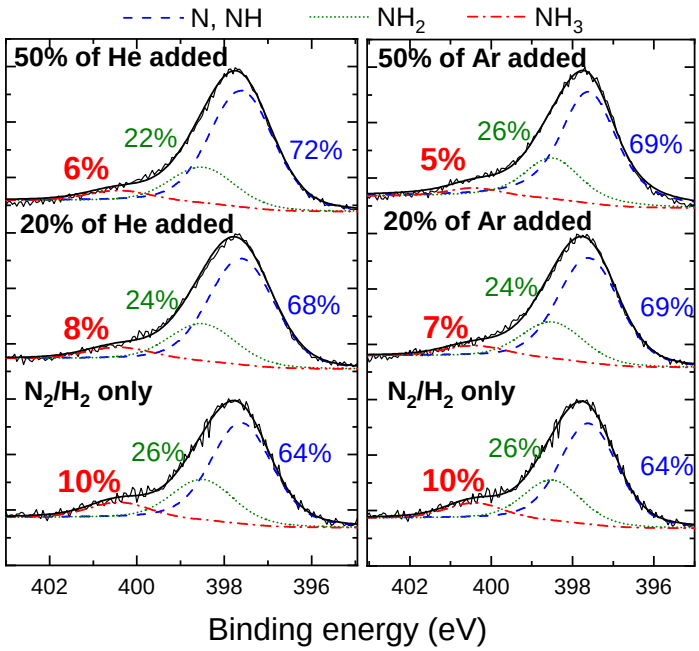

Figure 8: N1s core levels spectra recorded after pure N_2/H_2 as well as N_2/H_2/Ar or He plasma exposure of the W surface at RT. The red (dashdotted), green (shortly dotted) and blue (dashed) curves are the individual chemical states. Solid black curves are the raw data and the sum curves.

N1s core level peaks were decomposed into three singulets attributed to N and NH (at 397.6 eV), NH_2 (at 398.5 eV) and NH_3 (at 400.4 eV) [13]. The existence of surface nitrides on a W exposed sample to nitrogen-hydrogen plasma was also confirmed by the W4f core level peaks presented in our previous paper (see WN and WN_2 peaks in Figure 6 of paper [14]).

The percentages shown on the Figure 8 represent the ratio of N/NH, NH_2 and NH_3 from the total nitrogen atomic concentration on the surface. As can be seen, before the addition of the noble gas ammonia presents 10 at.% from the total nitrogen peak. This percentage decreases continuously by 40-50 % when Ar and He are added in equal ratio than nitrogen and hydrogen (50 % of the gas mixture P_{tot}). On the other hand, the N and NH ratio increased with the addition of He while NH_2 concentration decreases. However, the NH_2 peak is not affected much by Ar addition, and N/NH is not affected by further addition of Ar. It should be noted here that the nitrogen atomic concentration on the surface is almost unaffected by the addition of He (28 to 31 at.%) and Ar admixture (28 to 33 at.%).

4. Discussion

4.1. Plasma assisted ammonia catalysis at RT

Ammonia formation was observed both in the absence and presence of a catalyst in the chamber (Figure 2). It is still not clear if the production occurs in the plasma volume or on the quartz wall of the vacuum chamber. Based on previous studies [17–20], Hong et al. [21], summarized that ammonia can be produced at atmospheric pressure by three-body reactions between NH_x radicals (produced themselves by reactions between dissociated atoms and excited molecules) in the plasma phase. In a glow discharge microwave plasma, Uyama et al. [22, 23], stated the role of the volume reaction between NH radicals formed in the plasma volume and H_2 molecules on the ammonia formation. Recently, chemical kinetics modeling studies [17, 24] revealed that the gas phase volume reactions alone are not able to produce ammonia in detectable amounts. Taking these results into account and our measurements, we can attribute the production of ammonia without catalyst to either production in the plasma volume or recombination of dissociated species in the plasma on the quartz tube.

When W and SS catalytic surfaces were loaded, the ammonia production strongly increased (Figure 2). This was also reported in the PhD thesis of Patil [25] who studied the effect of Al_2O_3 supported metals and metal oxide catalysts on the ammonia formation in a DBD reactor. He showed that, with the presence of a catalytic surface, the ammonia production is around 3 times higher compared to the blank experiment where no surface is loaded in the quartz tube. In a more recent study, Shah et al [24] investigated the ammonia formation in an RF quartz plasma reactor and showed that the insertion of metal meshes catalysts in the quartz reactor highly increased the yield, in particular, on Au surface when 300 W of RF power was applied (5 times higher ammonia yield than without catalyst).

In our previous study [14], we showed that this increase was caused by the improvement of both the nitrogen cracking and the species interaction on the surface. By comparing the performance of both catalysts towards NH_3 synthesis, we can see that the tungsten surface acts as a better catalytic surface than SS for X_{N_2} above 10 %. Even though the SS surface contains predominantly iron (around 70 % of the total composition), known as the best catalyst for ammonia synthesis under thermal condition (see volcano plot in [26]), its lower production than W can be explained by the existence of other metals such as chromium (16 %) which have lower activity than Fe [27] or the presence of a native oxide layer. In fact, for SS, the surface is covered with a chromium oxide film that passivates the surface of the steel. This Cr_2O_3 oxide is typically a few nm thick [28] and it is not clear, in our case, if the argon plasma cleaning is removing the oxide as the sample is floating and if the hydrogen/nitrogen plasma is reducing the oxide layer to have an iron catalyst. Another factor that could also explain this difference between W and SS catalysts is the plasma effect on the catalytic activities of surfaces. In fact, Mehta et al. [29] showed, experimentally and through a microkinetic model, that the nitrogen excitation in the plasma changes the catalytic activity trends from

those known in thermal catalysis. In thermal catalysis, the best catalyst for ammonia presents an intermediate nitrogen binding energy i.e not not high to avoid having a strong nitrogen bond on the catalyst and consequent low reactivity and not too low to be able to dissociate the nitrogen. The presence of the plasma in catalysis produces excited nitrogen molecules with higher internal energy and lower dissociation barrier. Ammonia production is therefore maximized on catalysts that bind nitrogen weaker than those most active for thermal catalysis because they have smaller barriers for the hydrogenation of NH_x (x = 0,1,2) intermediates.

As can be seen in Figure 2, the maximum in NH_3 production is reached for different X_{N_2} depending on the presence of absence of a catalyst. Without catalyst, the maximum production corresponds to the stoichiometric mixture of nitrogen-hydrogen (25/75 % of N_2/H_2). This was also observed by Uyama and Matsumoto [30] who performed an N_2/H_2 microwave discharge in a Pyrex tube and also by Amorim et al. [31] through their DC glow discharge. When the catalyst was introduced, the maximum production shifts from the stoichiometry to a higher nitrogen content. Although the exact reason is still not clear, this shift was reported in several papers [29,32–35].

4.2. Plasma assisted ammonia catalysis at high temperature

Unlike on SS and W surfaces, the ammonia formed without a catalyst is almost constant for an increasing the temperature up to 900 K(Figure 3). The decrease starts at high temperature that corresponds to the decomposition temperature shown in Figure 4. This would suggest that, the quartz tube is not playing a catalytic role (as discussed in 4.1) and that most likely the ammonia formed without the catalyst is predominantly in the plasma. The decrease of the production of NH_3 on W and SS with increasing temperature, shown in Figure 3, can be attributed to several causes: (i) increased desorption of N_2 as the temperature is increased (ii) formation of more stable nitrides that react less with hydrogen to form ammonia (iii) ammonia thermal decomposition (iv) nitrogen continuous diffusion in the catalyst bulk leading to its decrease in the gas phase.
Note here that the focus is on the nitrogen (and not hydrogen) interaction with the surface as we have shown in previous work that the ammonia is formed, under these conditions, as a reaction between adsorbed nitrogen on the surface and hydrogen in the gas phase.

The first hypothesis (i) can be disproved by the XPS results in Figure 5. Indeed, the total nitrogen content on the surface is almost constant (in the range of 26-34 at.%) meaning that the decrease in the ammonia peak cannot be caused by a decrease in the nitrogen content on the surface with temperature. Previous studies have reported that the nitrogen release from W occurs only at high temperature in the range of 850 to 970 K [5,36]. However, the decrease in the NH_3 and NH_2 peak and increase in the N/NH peak suggest that a surface temperature increase leads to the formation of more stable nitrides that react less with the hydrogen to form ammonia, confirming hypothesis (ii).

At high temperatures (650 K for SS and 830 K for W), the decrease in the production can be well attributed to the thermal catalytic decomposition (iii) of the formed ammonia as shown in Figure 4. Thermal catalytic decomposition of ammonia is known as the reverse reaction of the Haber-Bosch synthesis of ammonia, one of the most extensively researched processes over the past 150 years [37]. Upon heating, ammonia decomposes to nitrogen and hydrogen through the following reaction: $2NH_3 \rightleftharpoons N_2 + 3H_2$
This reaction takes place in the gas phase, but it is strongly enhanced by the presence of a catalytic surface. Particularly over metals, the decomposition of ammonia occurs in a stepwise sequence of dehydrogenation reactions. These reactions are initiated by the adsorption of ammonia onto the active sites of the surface. The adsorbed molecules undergo then successive N–H bond cleavage, releasing hydrogen atoms that can combine to form molecular hydrogen. In the final step, nitrogen atoms recombine and desorb as molecular nitrogen [38, 39]. As shown in Figure 4b the ammonia decomposes with a fast rate to nitrogen and hydrogen on the W surface at 830 K. These observations are slightly different from the results of Markelj et al. [10] who studied the ammonia decomposition by flowing the gas through a hot tungsten capillary. For them, the dominant decomposition on W starts at lower temperature at about 680 K, attains the fastest increase at about 910 K and terminates around 1110 K. This discrepancy from our results could be attributed to the gas pressure difference. Previous studies [40, 41] performed at high temperature and on tungsten surface showed that the ammonia decomposition rate increases with its partial pressure. While Markelj et al. introduced the NH_3 gas at 2.7×10^{-1} mbar inside the capillary, a much lower pressure of 5×10^{-3} mbar was used in our setup which could explain the temperature shift where ammonia starts to decompose. On the other hand, the complete decomposition of ammonia at high temperature as well as the activation energy (Ea) of the reaction (1.05 $\pm$0.04 eV) are in a good agreement with their findings (1.07 $\pm$0.08 eV). The Ea was calculated by plotting the RGA peaks intensities in a logarithmic scale versus inverse temperature values, known as the Arrhenius plot (presented in the inset Figure 4). The curve was then fitted linearly and the activation energy was extracted from the slope according to the formula $R=A \times \exp(-Ea/k_B \times T)$ where R is the rate of the decomposition reaction, A is the pre-exponential factor, k_B is the Boltzmann constant and T is the measured temperature (more details about this method can be found in [10]).

Concerning the SS surface (Figure 4c), the ammonia decomposition presents a particular trend. The decomposition starts at lower temperature than on W surface and the release of the nitrogen is shifted to higher temperature values. This shift can be caused by the diffusion of the nitrogen and formation of stable nitrides with iron for temperature below 650 K (when ammonia start to decompose to nitrogen and hydrogen). This process is well known in the industry as the nitridation process where iron forms stable nitrides after exposure to ammonia at high temperature around 870 K [39, 42]. However, it has also been reported to start from temperatures as low as 570 K [26, 43].

This deactivation process is reversible at high reaction temperatures where desorption of the nitrogen takes place [39]. Note here that, the reason for ammonia peak rise between 900 K and 1050 K on the SS surface is still unknown.
The order of the activity of both catalysts (SS and W) is, therefore, reversed from ammonia synthesis to ammonia decomposition. Interestingly, even though the decomposition of ammonia is the reverse reaction of the synthesis, catalysts were shown in another study by Boisen et al. not to necessarily exhibit the same activity in both directions due to the difference in conditions and rate limiting steps [44].
It is also worth mentioning for the three thermal decomposition experiments without catalyst, on W and on SS, that ratios between ammonia peaks at 17, 16, 15 and 14 amu were constant and equal to the ammonia cracking pattern indicating therefore no release of the intermediate production of ammonia decomposition (NH_2 or NH) from the surface.

To sum up on the impact of temperature on ammonia production, we can conclude that the decrease is due to two major effects. For high temperatures ($T_{Surf} > 650$ K and 830 K for SS and W, respectively) the decrease in the production rate results from the thermal decomposition of ammonia. For lower temperature the temperature increase favor the formation of more stable nitrides that does not tend to react further with hydrogen to form NH_2 and NH_3. The possibility of bulk diffusion of the nitrogen cannot be rejected also and further thermal desorption experiments are required to quantify the trapped nitrogen.

4.3. He and Ar effect

To our knowledge, only two groups [9, 11] were interested in the study of Ar and He effect on ammonia formation and there is still considerable disagreement between their results. Experiments performed in the linear plasma device (GyM), using a microwave sustained N_2/D_2 plasma, show a reduction of 80 % in the ammonia production when 17 % of He was added while the addition of 3.1 % of Ar to the hydrogen nitrogen mixture was almost not effective. This effect was attributed to a modification of the physical-chemical process on the surface where helium acts as a barrier for the ammonia formation by occupying the catalyst active sites. On the other hand, the other group [11] reported an increase by 45 % of the produced NH_3 for only 8 % of added He. According to them, the increased ammonia formation with the He addition does not result from a higher adsorption of active species on the surface but rather due to an enhancement of the N-H recombination induced by the helium bombardment. In both studies, the authors confirm the need for further experiments to investigate the surface state and species in order to support their explanation. In this context, surface analysis of the exposed surface to a N_2/H_2/Ar or He plasma were performed in this manuscript.

When He and Ar are added to N_2/H_2, XPS measurements of the W surface (Figure 8) show a drop in the ammonia peak and a rise in the N/NH peak while the total surface nitrogen atomic concentration was constant. These observations indicate that

the presence of the two noble gases does not inhibit the adsorption of nitrogen on the W catalyst (a key step for the ammonia formation) but is rather unfavorable for the hydrogen and nitrogen surface recombination to form NH_3 from the surface nitrides. It should be mentioned here that conclusions from XPS are restricted to species on the surface and do not consider what was formed and desorbed as compounds.

The slight increase in the ammonia production with argon addition can be explained by the generation of more active nitrogen species. Hong et al. [45] investigated this effect by adding 10 sccm of Ar to 30 sccm of N_2 and 30 sccm of H_2 feed gas stream in a dielectric-barrier discharge reactor. They observed an increase in the discharge power, uniformity and gas temperature, and those factors lead to higher ammonia production rates. The optical emission spectra also indicated an increase in N^+ possibly resulting from a reaction between Ar^+ and N_2. This increase in nitrogen dissociated atoms contributed therefore to the increase in NH_3 production. Nakajima et al. [46] further explained further this reaction between nitrogen and ionized argon as a charge transfer reaction followed by dissociative recombination of nitrogen with an electron from the plasma:

$$N_2 + Ar^+ \longrightarrow N_2^+ + Ar$$
$$N_2^+ + e^- \longrightarrow N + N$$

The charge transfer reaction between nitrogen and argon is favoured by the fact that both species have almost the same ionization energy shown in table 2. However, when He is added to the mixture this reaction is not expected to occur due to the high ionization energy of helium.

Species	H_2	N_2	He	Ar
First ionization energy (eV)	15.42	15.58	24.56	15.76

Table 2: first ionization energies of nitrogen, hydrogen, helium and argon

A further explanation of the argon and helium effects can be related to the change of the electron temperature of electron density, key parameters in the generation of active species for the formation of ammonia. As shown in Figure 7, both gases show opposite effects on both T_e and n_e. These effects were already reported by Mansour et al. [47] and by Pu et al. [48] for adding He and Ar in pure N_2 plasma. Pu et al. explained these results in the following way. The electron energy distribution function in a plasma shows a tail region populated by high energy ("hot") electrons with energies above 30 eV. In the helium–nitrogen mixture, the tail is generated by He metastable states and superelastic collisions and is enlarged by adding more helium in the discharge. As a result, T_e increases. However, when argon is added in the discharge, there is a sharp increase in electron density and hence a higher electron-electron collision frequency, which always tend to deplete electrons in the "hot tail" and decrease T_e. In the case of Ar in an H_2 plasma, Sode et al. [49] show that T_e decreases monotonically and they

attributed the observed decrease to the increasing effective ion mass with increasing Ar fraction. As described by El-Sayed et al. [50], Ar can induce the dissociation of molecular nitrogen and increase the production of nitrogen atoms, however it has an insignificant effect on the nitrogen ionization mechanism. On the other hand, He addition enhances the production of, N^+ and N^- atoms through ionization, ionization dissociation and dissociative reaction, however it has a decreasing effect on the dissociative recombination mechanism.

In summary, on the catalyst surface, both He and Ar were to shown unfavorable impact on the hydrogen and nitrogen surface recombination to form NH_3. This effect, along with a high increase in the the electron temperature, is predominant when helium is added resulting in a total decrease of ammonia produced from the interaction of the plasma with the catalyst measured by RGA. Argon addition, on the other hand, was shown to increase the active nitrogen species in the plasma and, as a consequence, the percentage of ammonia formed. In this case, the competition between the ammonia increase in the plasma and the decrease on the surface results in a total increase of the production when a W catalyst is used.

5. Conclusion

In this study, we explored the formation of ammonia from an N_2/H_2 RF plasma both without and with tungsten and stainless steel catalysts for different X_{N_2}. We demonstrated that the presence of the catalytic surface highly increases the ammonia formation rate.

An increase of the surface temperature results in a decrease in the ammonia formation rate due to two factors. For high temperatures above 650 K and 830 K for SS and W, respectively, the production decrease is caused by the thermal decomposition of ammonia. At lower temperature, the temperature increase leads to the formation of stable nitrides that do not tend to react further with hydrogen to form NH_2 and NH_3. These results imply that in the tokamak, the high temperature active area of the W divertor (where plasma impact occurs) and its surrounding will not contribute much in the ammonia production. As the NH_3 formation is favored by low temperature, a high contribution from the plasma shaded areas is expected.

Finally, we have shown that the addition of helium and argon to the nitrogen-hydrogen plasma have opposite effects on the ammonia production. While He effectively decreases the percentage of NH_3 by acting as a barrier for the surface processes, argon impacts more the plasma processes by increasing the active nitrogen species in the plasma and, as a consequence, the percentage of ammonia formed. This suggests that the presence of He as an intrinsic impurity in the fusion plasma might help to decrease the ammonia production and could further be used in a mixture with the nitrogen seeding gas. In contrary, it is not a good option to mix nitrogen and argon together to decrease the ammonia formation.

6. Acknowledgements

This work has been carried out within the framework of the EUROfusion Consortium and has received funding from the Euratom research and training program 2014-2018 and 2019-2020 under grant agreement No 633053. The views and opinions expressed herein do not necessarily reflect those of the European Commission or of the ITER Organization. ITER is the Nuclear Facility INB no. 174. This paper applies new physics analysis related to tritiated ammonia formation which is not yet incorporated into the ITER technical baseline. The nuclear operator is not constrained by the results presented here. The authors would like to thank the Swiss Federal Office of Energy, the Swiss Nanoscience Institute, the Swiss National Science Foundation and the Federal Office for Education and Science for their financial support.

7. References

[1] D. Neuwirth, V. Rohde, T. Schwarz-Selinger, and A. U. Team, "Formation of ammonia during nitrogen-seeded discharges at asdex upgrade," *Plasma Physics and Controlled Fusion*, vol. 54, no. 8, p. 085008, 2012.

[2] A. Kallenbach, M. Bernert, R. Dux, L. Casali, T. Eich, L. Giannone, A. Herrmann, R. McDermott, A. Mlynek, H. Müller *et al.*, "Impurity seeding for tokamak power exhaust: from present devices via iter to demo," *Plasma Physics and Controlled Fusion*, vol. 55, no. 12, p. 124041, 2013.

[3] V. Rohde, M. Oberkofler *et al.*, "Ammonia production in nitrogen seeded plasma discharges in asdex upgrade," *Journal of Nuclear Materials*, vol. 463, pp. 672–675, 2015.

[4] M. Oberkofler, G. Meisl, A. Hakola, A. Drenik, D. Alegre, S. Brezinsek, R. Craven, T. Dittmar, T. Keenan, S. Romanelli *et al.*, "Nitrogen retention mechanisms in tokamaks with beryllium and tungsten plasma-facing surfaces," *Physica Scripta*, vol. 2016, no. T167, p. 014077, 2016.

[5] M. Oberkofler, D. Alegre, F. Aumayr, S. Brezinsek, T. Dittmar, K. Dobes, D. Douai, A. Drenik, M. Köppen, U. Kruezi *et al.*, "Plasma–wall interactions with nitrogen seeding in all-metal fusion devices: Formation of nitrides and ammonia," *Fusion engineering and design*, vol. 98, pp. 1371–1374, 2015.

[6] A. Drenik, D. Alegre, S. Brezinsek, A. de Castro, U. Kruezi, G. Meisl, M. Mozetic, M. Oberkofler, M. Panjan, G. Primc *et al.*, "Detection of ammonia by residual gas analysis in aug and jet," *Fusion Engineering and Design*, vol. 124, pp. 239–243, 2017.

[7] A. Drenik, L. Laguardia, R. M. McDermott, G. Meisl, R. Neu, M. Oberkofler, E. Pawelec, R. A. Pitts, S. Potzel, T. Pütterich *et al.*, "Evolution of nitrogen concentration and ammonia production in n-2-seeded h-mode discharges at asdex upgrade," *Nuclear Fusion*, vol. 59, no. 4, 2019.

[8] M. Oberkofler, D. Douai, S. Brezinsek, J. Coenen, T. Dittmar, A. Drenik, S. Romanelli, E. Joffrin, K. McCormick, M. Brix *et al.*, "First nitrogen-seeding experiments in jet with the iter-like wall," *Journal of Nuclear Materials*, vol. 438, pp. S258–S261, 2013.

[9] L. Laguardia, R. Caniello, A. Cremona, G. Gatto, G. Gervasini, F. Ghezzi, G. Granucci, V. Mellera, D. Minelli, R. Negrotti *et al.*, "Influence of he and ar injection on ammonia production in n2/d2 plasma in the medium flux gym device," *Nuclear Materials and Energy*, vol. 12, pp. 261–266, 2017.

[10] S. Markelj, A. Založnik, and I. Čadež, "Interaction of ammonia and hydrogen with tungsten at elevated temperature studied by gas flow through a capillary," *Journal of Vacuum Science & Technology A: Vacuum, Surfaces, and Films*, vol. 35, no. 6, p. 061602, 2017.

[11] A. de Castro, D. Alegre, and F. Tabarés, "Influence of residence time and helium addition in the

ammonia formation on tungsten walls in n2h2 glow discharge plasmas," *Nuclear Materials and Energy*, vol. 12, pp. 399–404, 2017.

[12] R. Pitts, S. Carpentier, F. Escourbiac, T. Hirai, V. Komarov, S. Lisgo, A. Kukushkin, A. Loarte, M. Merola, A. S. Naik *et al.*, "A full tungsten divertor for iter: Physics issues and design status," *Journal of Nuclear Materials*, vol. 438, pp. S48–S56, 2013.

[13] M. B. Yaala, L. Marot, R. Steiner, L. Moser, G. De Temmerman, C. Porosnicu, C. Lungu, M. Oberkofler, and E. Meyer, "Quartz micro-balance and in situ xps study of the adsorption and decomposition of ammonia on gold, tungsten, boron, beryllium and stainless steel surfaces," *Nuclear Fusion*, vol. 58, no. 10, p. 106012, 2018.

[14] M. Ben Yaala, A. Saeedi, D.-F. Scherrer, L. Moser, R. Steiner, M. Zutter, M. Oberkofler, G. De Temmerman, L. Marot, and E. Meyer, "Plasma-assisted catalytic formation of ammonia in n 2–h 2 plasma on a tungsten surface," *Physical Chemistry Chemical Physics*, vol. 21, no. 30, pp. 16 623–16 633, 2019.

[15] S. Iyyakkunnel, L. Marot, B. Eren, R. Steiner, L. Moser, D. Mathys, M. Duggelin, P. Chapon, and E. Meyer, "Morphological changes of tungsten surfaces by low-flux helium plasma treatment and helium incorporation via magnetron sputtering," *ACS applied materials & interfaces*, vol. 6, no. 14, pp. 11 609–11 616, 2014.

[16] S. Tougaard, "Accuracy of the non-destructive surface nanostructure quantification technique based on analysis of the xps or aes peak shape," *Surface and Interface Analysis: An International Journal devoted to the development and application of techniques for the analysis of surfaces, interfaces and thin films*, vol. 26, no. 4, pp. 249–269, 1998.

[17] E. Carrasco, M. Jiménez-Redondo, I. Tanarro, and V. J. Herrero, "Neutral and ion chemistry in low pressure dc plasmas of h 2/n 2 mixtures: routes for the efficient production of nh3 and nh 4+," *Physical Chemistry Chemical Physics*, vol. 13, no. 43, pp. 19 561–19 572, 2011.

[18] J. Hong, S. Pancheshnyi, E. Tam, J. J. Lowke, S. Prawer, and A. B. Murphy, "Kinetic modelling of nh3 production in n2–h2 non-equilibrium atmospheric-pressure plasma catalysis," *Journal of Physics D: Applied Physics*, vol. 50, no. 15, p. 154005, 2017.

[19] H. Uyama and O. Matsumoto, "Reaction scheme of ammonia formation in microwave-discharge from quenching reactions of nh radicals by hydrogen," *Denki Kagaku*, vol. 61, no. 7, pp. 925–926, 1993.

[20] M. L. Steen, K. R. Kull, and E. R. Fisher, "Comparison of surface interactions for nh and nh 2 on polymer and metal substrates during nh 3 plasma processing," *Journal of applied physics*, vol. 92, no. 1, pp. 55–63, 2002.

[21] J. Hong, S. Prawer, and A. B. Murphy, "Plasma catalysis as an alternative route for ammonia production: Status, mechanisms, and prospects for progress," *ACS Sustainable Chemistry & Engineering*, vol. 6, no. 1, pp. 15–31, 2017.

[22] H. Uyama and O. Matsumoto, "Synthesis of ammonia in high-frequency discharges. ii. synthesis of ammonia in a microwave discharge under various conditions," *Plasma Chemistry and Plasma Processing*, vol. 9, no. 3, pp. 421–432, 1989.

[23] O. Uyama, Haruo; Matsumoto, "Synthesis of ammonia in high-frequency discharges." in *Proceedings of the Tenth International Symposium on Plasma Chemistry (ISPC-10), Bochum, Germany*, no. sect. 2.3–10, Aug. 1991, p. 1.

[24] J. Shah, W. Wang, A. Bogaerts, and M. L. Carreon, "Ammonia synthesis by radio frequency plasma catalysis: revealing the underlying mechanisms," *ACS Applied Energy Materials*, vol. 1, no. 9, pp. 4824–4839, 2018.

[25] B. Patil, "Plasma (catalyst)-assisted nitrogen fixation: reactor development for nitric oxide and ammonia production," Ph.D. dissertation, 2017.

[26] F. Schüth, R. Palkovits, R. Schlögl, and D. S. Su, "Ammonia as a possible element in an energy infrastructure: catalysts for ammonia decomposition," *Energy & Environmental Science*, vol. 5, no. 4, pp. 6278–6289, 2012.

[27] J. C. Ganley, F. Thomas, E. Seebauer, and R. I. Masel, "A priori catalytic activity correlations:

the difficult case of hydrogen production from ammonia," *Catalysis Letters*, vol. 96, no. 3-4, pp. 117–122, 2004.

[28] S. Tardio, M.-L. Abel, R. H. Carr, J. E. Castle, and J. F. Watts, "Comparative study of the native oxide on 316l stainless steel by xps and tof-sims," *Journal of Vacuum Science & Technology A: Vacuum, Surfaces, and Films*, vol. 33, no. 5, p. 05E122, 2015.

[29] P. Mehta, P. Barboun, F. A. Herrera, J. Kim, P. Rumbach, D. B. Go, J. C. Hicks, and W. F. Schneider, "Overcoming ammonia synthesis scaling relations with plasma-enabled catalysis," *Nature Catalysis*, vol. 1, no. 4, p. 269, 2018.

[30] H. Uyama and O. Matsumoto, "Synthesis of ammonia in high-frequency discharges," *Plasma chemistry and plasma processing*, vol. 9, no. 1, pp. 13–24, 1989.

[31] J. Amorim, G. Baravian, and G. Sultan, "Absolute density measurements of ammonia synthetized in n2–h2 mixture discharges," *Applied physics letters*, vol. 68, no. 14, pp. 1915–1917, 1996.

[32] T. Mizushima, K. Matsumoto, H. Ohkita, and N. Kakuta, "Catalytic effects of metal-loaded membrane-like alumina tubes on ammonia synthesis in atmospheric pressure plasma by dielectric barrier discharge," *Plasma Chemistry and Plasma Processing*, vol. 27, no. 1, pp. 1–11, 2007.

[33] T. Body, S. Cousens, J. Kirby, and C. Corr, "A volume-averaged model of nitrogen–hydrogen plasma chemistry to investigate ammonia production in a plasma-surface-interaction device," *Plasma Physics and Controlled Fusion*, vol. 60, no. 7, p. 075011, 2018.

[34] A. Gómez-Ramírez, J. Cotrino, R. Lambert, and A. González-Elipe, "Efficient synthesis of ammonia from n2 and h2 alone in a ferroelectric packed-bed dbd reactor," *Plasma Sources Science and Technology*, vol. 24, no. 6, p. 065011, 2015.

[35] H.-H. Kim, Y. Teramoto, A. Ogata, H. Takagi, and T. Nanba, "Atmospheric-pressure nonthermal plasma synthesis of ammonia over ruthenium catalysts," *Plasma Processes and Polymers*, vol. 14, no. 6, p. 1600157, 2017.

[36] X. Zhang, Y. Wu, B. Mu, L. Qiao, W. Li, J. Li, and P. Wang, "Thermal stability of tungsten sub-nitride thin film prepared by reactive magnetron sputtering," *Journal of Nuclear Materials*, vol. 485, pp. 1–7, 2017.

[37] A. K. Hill and L. Torrente-Murciano, "Low temperature h2 production from ammonia using ruthenium-based catalysts: Synergetic effect of promoter and support," *Applied Catalysis B: Environmental*, vol. 172, pp. 129–135, 2015.

[38] D. A. Hansgen, D. G. Vlachos, and J. G. Chen, "Using first principles to predict bimetallic catalysts for the ammonia decomposition reaction," *Nature chemistry*, vol. 2, no. 6, p. 484, 2010.

[39] T. Bell and L. Torrente-Murciano, "H2 production via ammonia decomposition using non-noble metal catalysts: a review," *Topics in Catalysis*, vol. 59, no. 15-16, pp. 1438–1457, 2016.

[40] K. Tamaru, "A" new" general mechanism of ammonia synthesis and decomposition on transition metals," *Accounts of Chemical Research*, vol. 21, no. 2, pp. 88–94, 1988.

[41] S. Mukherjee, S. V. Devaguptapu, A. Sviripa, C. R. Lund, and G. Wu, "Low-temperature ammonia decomposition catalysts for hydrogen generation," *Applied Catalysis B: Environmental*, vol. 226, pp. 162–181, 2018.

[42] L. Marot, L. Pichon, M. Drouet, and A. Straboni, "Improved nitrogen transport in fe–c alloys during nh3 plasma nitridation," *Materials Letters*, vol. 44, no. 1, pp. 35–38, 2000.

[43] L. Marot, E. Le Bourhis, and A. Straboni, "Improved nitridation efficiency and mechanical property of stainless steel surface after n2–h2 plasma nitridation at low temperature," *Materials letters*, vol. 56, no. 1-2, pp. 76–79, 2002.

[44] A. Boisen, S. Dahl, J. K. Nørskov, and C. H. Christensen, "Why the optimal ammonia synthesis catalyst is not the optimal ammonia decomposition catalyst," *Journal of Catalysis*, vol. 230, no. 2, pp. 309–312, 2005.

[45] J. Hong, S. Prawer, and A. B. Murphy, "Production of ammonia by heterogeneous catalysis in a packed-bed dielectric-barrier discharge: influence of argon addition and voltage," *IEEE Transactions on Plasma Science*, vol. 42, no. 10, pp. 2338–2339, 2014.

[46] J. Nakajima and H. Sekiguchi, "Synthesis of ammonia using microwave discharge at atmospheric

pressure," *Thin Solid Films*, vol. 516, no. 13, pp. 4446–4451, 2008.

[47] M. Mansour, N. El-Sayed, O. Farag, and M. Elghazaly, "Effect of he and ar addition on n2 glow discharge characteristics and plasma diagnostics," *Arab J. of Nuclear Sci. and Applications*, vol. 46, no. 1, pp. 116–125, 2013.

[48] Y.-K. Pu, Z.-G. Guo, Z.-D. Kang, J. Ma, Z.-C. Guan, G.-Y. Zhang, and E.-G. Wang, "Comparative characterization of high-density plasma reactors using emission spectroscopy from vuv to nir," *Pure and applied chemistry*, vol. 74, no. 3, pp. 459–464, 2002.

[49] M. Sode, T. Schwarz-Selinger, and W. Jacob, "Ion chemistry in h2-ar low temperature plasmas," *Journal of Applied Physics*, vol. 114, no. 6, p. 063302, 2013.

[50] N. Elsayed and o. farag, "The influence of the gas mixing ratio on some characteristics and reaction rate coefficients of ar/n2 and he/n2 dc plasma," *Arab Journal of Nuclear Sciences and Applications*, vol. 52, pp. 181–186, 04 2019.